Calpain 1 and 2 Are Required for RNA Replication of Echovirus 1[▽]

Paula Upla,[1] Varpu Marjomäki,[1] Liisa Nissinen,[2] Camilla Nylund,[4] Matti Waris,[3]
Timo Hyypiä,[3] and Jyrki Heino[4*]

Nanoscience Center/Department of Biological and Environmental Science, University of Jyväskylä, FI-40351 Jyväskylä, Finland[1];
Biotie Therapies, FI-20520 Turku, Finland[2]; Department of Virology, University of Turku, FI-20520 Turku, Finland[3]; and
Department of Biochemistry and Food Chemistry, University of Turku, FI-20520 Turku, Finland[4]

Calpains are calcium-dependent cysteine proteases that degrade cytoskeletal and cytoplasmic proteins. We have studied the role of calpains in the life cycle of human echovirus 1 (EV1). The calpain inhibitors, including calpeptin, calpain inhibitor 1, and calpain inhibitor 2 as well as calpain 1 and calpain 2 short interfering RNAs, completely blocked EV1 infection in the host cells. The effect of the inhibitors was not specific for EV1, because they also inhibited infection by other picornaviruses, namely, human parechovirus 1 and coxsackievirus B3. The importance of the calpains in EV1 infection also was supported by the fact that EV1 increased calpain activity 3 h postinfection. Confocal microscopy and immunoelectron microscopy showed that the EV1/caveolin-1-positive vesicles also contain calpain 1 and 2. Our results indicate that calpains are not required for virus entry but that they are important at a later stage of infection. Calpain inhibitors blocked the production of EV1 particles after microinjection of EV1 RNA into the cells, and they effectively inhibited the synthesis of viral RNA in the host cells. Thus, both calpain 1 and calpain 2 are essential for the replication of EV1 RNA.

The human calpain family has 14 members, some of which are tissue specific, while others are ubiquitous (13, 33, 39). The two prototype calpains are calpain 1 (μ-calpain or calpain I) and calpain 2 (m-calpain or calpain II). They are both ubiquitous, and their target proteins seem to be the same. Their major difference is in their calcium requirement: calpain 1 needs much less Ca^{2+} (half-maximal activity, 3 to 50 μM) to be activated than calpain 2 (half-maximal activity, 400 to 800 μM). The activation of calpains is a complex process, and many factors in addition to calcium concentration may regulate it. For example, the presence of phospholipids lowers the Ca^{2+} levels required (1, 28). Despite the fact that calpains are expressed in all cell types, relatively little is known about their physiological roles. Calpain 1-deficient mice have a platelet dysfunction (4), but knocking down both calpain 1 and 2 simultaneously leads to an embryonic-lethal phenotype (2). Calpains have a large number of target proteins, which seems to reflect the fact that calpains participate in many different cellular functions. Many of the target molecules are actin-associated or cytoskeletal proteins, including α-fodrin, talin, paxillin, and vinculin (for a more complete list of about 30 proteins, see reference 13). In addition, calpains can degrade cytoplasmic domains of integrins (27). Therefore, it is not surprising that the regulation of cytoskeleton-membrane interactions is one of the most important functions proposed for calpains. They also may regulate integrin-related signaling by the degradation of focal adhesion kinase, protein kinase C, and RhoA (6, 8, 21, 22, 31). The fact that calpains can remodel the cytoskeleton also potentially makes them important in vesicular trafficking in cells. However, very little is known about their participation in these processes.

Echovirus 1 (EV1) is a member of the family *Picornaviridae*, which comprises one of the largest and most important families of both human and animal pathogens, including polioviruses and foot-and-mouth disease viruses. Picornaviruses share similar icosahedral capsid structures that enclose a single-stranded, infectious RNA genome. EV1 uses α2β1 integrin, a collagen receptor, to bind to the cell surface (5), and we have shown previously that the virus enters the target cell in complex with its receptor and becomes located in caveolin-1-positive structures, apparently caveosomes (23). Later, the EV1 RNA genome is released into the cytoplasm, and its translation and multiplication are initiated.

Picornavirus replication follows a strategy typical for positive-sense RNA viruses. Viral RNA is translated into a polyprotein that is cleaved by virus-encoded proteases. Many details of the kinetics and regulation of the cleavage events still are poorly understood. After the primary synthesis of viral proteins, picornaviruses initiate the replication of their genome through negative-strand RNA templates on cytoplasmic membranes of different origins. Viral nonstructural proteins, rather than RNA, are responsible for the targeting of the replication complex to the membranes (29).

There are only a few examples of calpains participating in virus infection. In monocytic cells latently infected with human immunodeficiency virus type 1 (HIV-1), viral replication stimulated by phorbol myristate acetate and calcium can be inhibited by calpain inhibitor 1 (34). The target of calpain cleavage is a cytoplasmic inhibitory molecule, IκBα, of the cellular transcription factor NF-κB. NF-κB triggers the transcription of viral genes, resulting in a massive increase in HIV-1 replication (34). Another example is hepatitis C virus infection, in which the cleavage of nonstructural protein NS5A is blocked by cal-

pain inhibitors 1 and 2 (18). NS5A not only participates in the modulation of virus replication but also affects many host cell functions (18).

Viruses, including picornaviruses, are capable of affecting the apoptotic machinery of the host cells. Reovirus, a nonenveloped, double-stranded RNA virus, causes a cytopathic effect by initiating the apoptosis in target cells (10). The reovirus-induced apoptosis is preceded by increased calpain activity that is blocked by calpain inhibitors (10). One possible explanation for the increased calpain activity in reovirus infection was suggested to be the calcium flux following viral attachment (10). Virus-induced elevations of cytosolic calcium levels also have been demonstrated in HIV-1 (26) and coxsackievirus (36) infections.

In this study, we show the pivotal role of calpain 1 and 2 in EV1 infection. Calpain activity increases in SAOS-α2β1 cells during EV1 infection, and both calpain 1 and calpain 2 are essential for the replication of EV1 RNA.

MATERIALS AND METHODS

Cells, viruses, and antibodies. SAOS cells (ATCC) stably transfected with an expression construct encoding α2 integrin (SAOS-α2β1 cells) (16), A549 cells (ATCC), GMK cells (ATCC), HeLa MZ cells (from Urs Greber, University of Zurich, Switzerland), and human kidney 293 cells (ATCC) were used in the experiments. EV1 (Farouk strain; ATCC) was propagated in GMK cells and purified in sucrose gradients as described previously (23), human parechovirus 1 (HPEV1) (15) was grown in A549 cells, and coxsackievirus B3 (CVB3) (Nancy strain) (37) was grown in LLC-MK$_2$ cells. Antisera against purified EV1 (23), HPEV1 (17), and CVB3 (37), as well as antiserum recognizing a conserved peptide sequence in CVB3 virus 3D RNA polymerase (3) that also was reactive with EV1 3D protein (M. Karjalainen, unpublished data), were produced in rabbits. The following antibodies against cellular structures were used: rabbit antisera against caveolin-1 (N-20; Santa Cruz and Transduction Laboratories), calpain 1 (Santa Cruz), and calpain 2 (Sigma), and monoclonal antibodies against the integrin α2 subunit (MCA2025; Serotec), HAS6 (a gift from Fiona M. Watt), caveolin-1 (Zymed), calpain 1 (Calbiochem), and tubulin (Sigma).

Plaque titration. SAOS-α2β1 cells that had been incubated in the presence or absence of 140 μM calpeptin were collected 8 h postinfection (p.i.), and after a freeze-thaw cycle, the samples were diluted from 10^{-4} to 10^{-8} in phosphate-buffered saline (PBS). The dilutions were incubated on confluent GMK cells at 37°C for 30 min, and the cells then were overlaid with carboxymethyl cellulose. The cells were incubated for 2 days prior to being stained with crystal violet, and then the plaques were counted.

Immunofluorescence and confocal microscopy. Subconfluent cell cultures (SAOS-α2β1, HeLa MZ, and 293 cells) were incubated with EV1 (multiplicity of infection, 100) for 1 h on ice, washed, and incubated at 37°C for various time periods in Dulbecco's modified essential medium (DMEM) containing 1% fetal calf serum (FCS). Subconfluent A549 cells were incubated with HPEV1 for 1 h at 4°C, washed, and incubated at 37°C for 6 h. Subconfluent SAOS-α2β1 and GMK cells were incubated with CVB3 for 1 h on ice, washed, and incubated at 37°C for 7 h. The cells were fixed with 4% paraformaldehyde for 20 min at room temperature and permeabilized with 0.2% Triton X-100. For calpain inhibition, calpeptin (140 μM; Calbiochem), calpain inhibitor 1, and calpain inhibitor 2 (130 μM each; Roche) were used. To monitor protease inhibition, SAOS-α2β1 cells were preincubated with the protease inhibitors antipain (Sigma), leupeptin (Sigma), aprotinin (Sigma), trypsin inhibitor (Sigma), and elastatinal (Sigma) at 37°C for 30 min, followed by EV1 infection in the presence of inhibitors. Highly cross-absorbed goat secondary antibodies against rabbit (Alexa red, 546 nm; Molecular Probes) and mouse (Alexa green, 488 nm; Molecular Probes) immunoglobulins (Ig) were used in the labelings. To detect glycosylphosphatidylinositol-anchored proteins (GPI-APs), the Alexa 546-conjugated mutant aerolysin (12) was used. For the triple immunofluorescence labeling, a Zenon rabbit IgG labeling kit (Molecular Probes) was used. The cells were mounted in Mowiol and examined with an Axiovert 100 M SP epifluorescence microscope (Carl Zeiss, Jena, Germany) equipped with a confocal setup (Zeiss LSM510). Images were acquired using a Plan Neofluar objective (×63 oil immersion; numerical aperture, 1.25) and a digital resolution of 512 by 512. False colocalization signals were avoided by scanning fluorescence from different excitation wavelengths separately.

Electron microscopy. For electron microscopy, SAOS-α2β1 cells were incubated with anti-α2 MAb (HAS6; 1:200) together with EV1 for 1 h on ice and washed. The cells subsequently were incubated with rabbit anti-mouse IgG antibody for 1 h on ice, washed, and treated with protein A-gold (10-nm-diameter particles; G. Posthuma and J. Slot, Utrecht, The Netherlands) also for 1 h on ice, followed by being washed. After that, the cells were incubated for 30 min at 37°C and washed once on ice. The cells were harvested in homogenizing buffer (3 mM imidazole, 0.25 M sucrose, 1 mM EDTA), pelleted (5,900 × g for 5 min), resuspended in homogenizing buffer, and homogenized by passing the pellet extensively through a 23-gauge needle. The cell lysate was bound on grids used in electron microscopy for 40 min at room temperature and blocked with 10% FCS for 15 min. The cell lysate samples then were incubated with primary antibodies in 5% FCS–PBS for 40 min, washed with PBS, coupled with protein A-gold (5-nm-diameter particles; G. Posthuma and J. Slot, Utrecht, The Netherlands), and washed again. The samples were fixed in 2.5% glutaraldehyde for 5 min, washed in H$_2$O, and coated with methylcellulose.

Measurement of internalization. The internalization of EV1 or integrin clusters was estimated by confocal microscopy using the 3D for LSM program, version 1.4.2 (Carl Zeiss, Jena, Germany). Cells were infected with EV1 alone or in combination with 140 μM calpeptin for 2 h and fixed with 3% paraformaldehyde for 15 min. After fixation, EV1 was labeled without permeabilization using a primary EV1 antiserum and then the anti-rabbit Alexa 546 conjugate. After a 5-min permeabilization with 0.2% Triton X-100, EV1 was labeled again, but this time the anti-rabbit Alexa 488 conjugate was used. Thus, plasma membrane-associated EV1 was stained with both Alexa 546 and Alexa 488 conjugates and seen as yellow when the red and green channels were merged, whereas green signal represented internalized EV1. The double-labeled cells were imaged as serial sections with confocal microscopy, and then the volume of internalized vesicles and the total amount of fluorescence was measured using the 3D for LSM program. In a parallel experiment, an antibody against α2 integrin, in the presence or absence of 140 μM calpeptin, was added to the medium, incubated for 1 h on ice and washed. The cells subsequently were incubated with Alexa 488-conjugated anti-mouse antibody with or without 140 μM calpeptin for 1 h on ice and then washed. The formation of integrin clusters was allowed to occur at 37°C for 2 h, and the samples were fixed as described above. The internalized integrins had a green color, and the plasma membrane-associated integrins were labeled with Alexa 546 conjugate. Again, yellow in merge images represented integrin clusters on the plasma membrane, and green signal represented internalized clusters. Altogether, 20 cells were measured in both experiments.

SDS-PAGE and immunoblotting. For sodium dodecyl sulfate-polyacrylamide gel electrophoresis (SDS-PAGE) and immunoblotting, cells were scraped from 2-ml dishes into Laemmli sample buffer, and then the samples were separated in a 10% polyacrylamide gel and electroblotted onto a polyvinylidene difluoride membrane (Millipore). Primary antibodies and horseradish peroxidase-conjugated secondary antibodies (Bio-Rad) were used. Bands were detected by chemiluminescence (Pierce).

Calpain activity. To activate calpain with 12-O-tetradecanoylphorbol-13-acetate (TPA), SAOS-α2β1 cells were plated on dishes and incubated for 3 h in serum-free medium. After that, TPA (100 ng/ml) was added and the incubation was continued for 5 min to determine the levels of calpain 1 and 2 by Western blot analysis using specific antibodies. For measuring calpain activity from detergent-soluble and -insoluble fractions, the incubation was continued for 5, 15, and 30 min, after which the cells were harvested and lysed in 0.1% Triton X-100 in Tris-HCl buffer. The lysates were centrifuged to separate detergent-soluble and -insoluble fractions, and subsequently calpain activity was measured (Tecan Group, Ltd.).

Metabolic labeling. Uninfected or EV1-infected SAOS-α2β1 cells, in the presence or absence of 140 μM calpeptin, were incubated in methionine/cysteine-deficient medium until 3 h p.i., after which [^{35}S]methionine label (100 μCi/ml; MP Biomedicals) was added to the medium. The cells were scraped 8 h p.i. and incubated with 100 mM octyl-β-D-glucopyranoside (30 min) on ice. Labeled viral proteins then were analyzed by SDS–10% PAGE.

Microinjection. SAOS-α2β1 cells on glass coverslips were washed and incubated in DMEM containing 1% FCS in the presence or absence of 140 μM calpeptin. Fifty cells were microinjected with EV1 RNA (isolated with a high pure RNA viral kit; Roche) and incubated at 37°C for 5 h.

In vitro translation. The in vitro translation reaction was performed according to the manufacturer's instructions (Retic lysate IV in vitro translation kit; Ambion). The components of the reaction mixture, including [^{S}35]methionine, were mixed in Eppendorf tubes, and 12 μg of EV1 RNA (isolated with a high pure RNA viral kit; Roche), with or without 140 μM calpeptin, was added on ice. The tubes were incubated at 30°C for 100 min in a water bath. The samples were
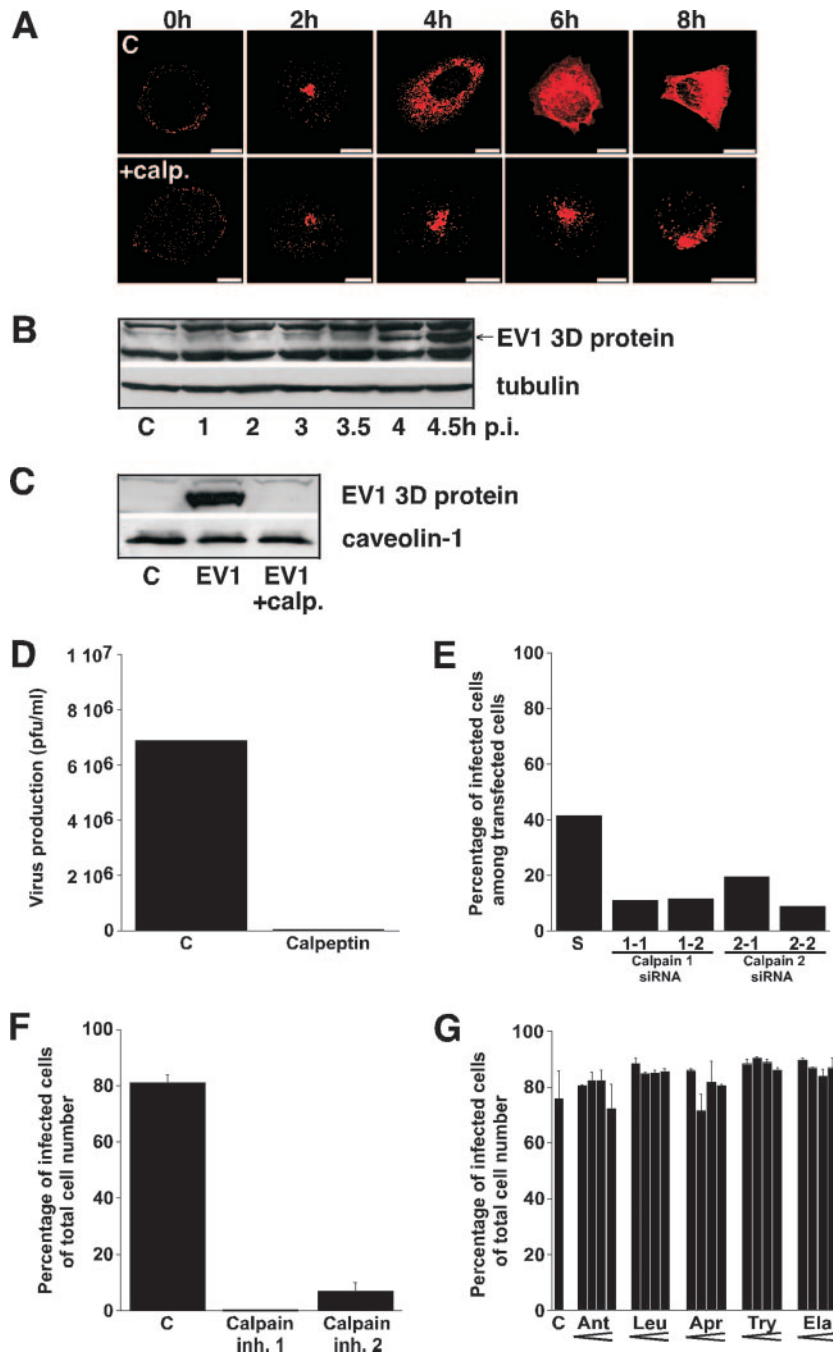
FIG. 1. Calpain inhibitors block EV1 infection. (A) Immunofluorescent labeling of SAOS-α2β1 cells infected with EV1, using virus-specific antiserum with or without calpeptin (calp.; 140 μM) treatment after viral attachment (0 h) or 2, 4, 6, and 8 h p.i. Images are of sections through the center area of the cells. Bars, 10 μm. (B) Western blot analysis of the time course of EV1 3D protein expression in SAOS-α2β1 cells. C, uninfected control. Anti-tubulin antibody was used as a loading control. (C) Western blot analysis of EV1 3D protein in SAOS-α2β1 cells 6 h p.i., with or without calpeptin (calp.; 140 μM) treatment. Anti-caveolin-1 antibody was used as a loading control. (D) Plaque titration assay showing the production of infectious EV1 in SAOS-α2β1 cells in the presence or absence of 140 μM calpeptin. (E) The number of EV1-infected cells 6 h p.i. among siRNA-positive cells was determined after siRNA transfection of calpain 1 (1-1 and 1-2) and 2 (2-1 and 2-2) siRNAs for 72 h. A scrambled (S) siRNA was used as a control. (F) Blocking effects of calpain inhibitor 1 and calpain inhibitor 2 on EV1 infection, determined 6 h p.i. in SAOS-α2β1 cells. Inh., inhibitor. (G) The effect of several protease inhibitors with increasing concentrations on EV1 infection in SAOS-α2β1 cells calculated 6 h p.i. The inhibitors used were antipain (Ant; 125, 250, 500, and 1,000 μM), leupeptin (Leu; 125, 250, 500, and 1,000 μM), aprotinin (Apr; 1.25, 2.5, 5, and 10 U/ml), trypsin inhibitor (Try; 0.5, 1, 2, and 4 mM), and elastatinal (Ela; 62.5, 125, 250, and 500 μM).
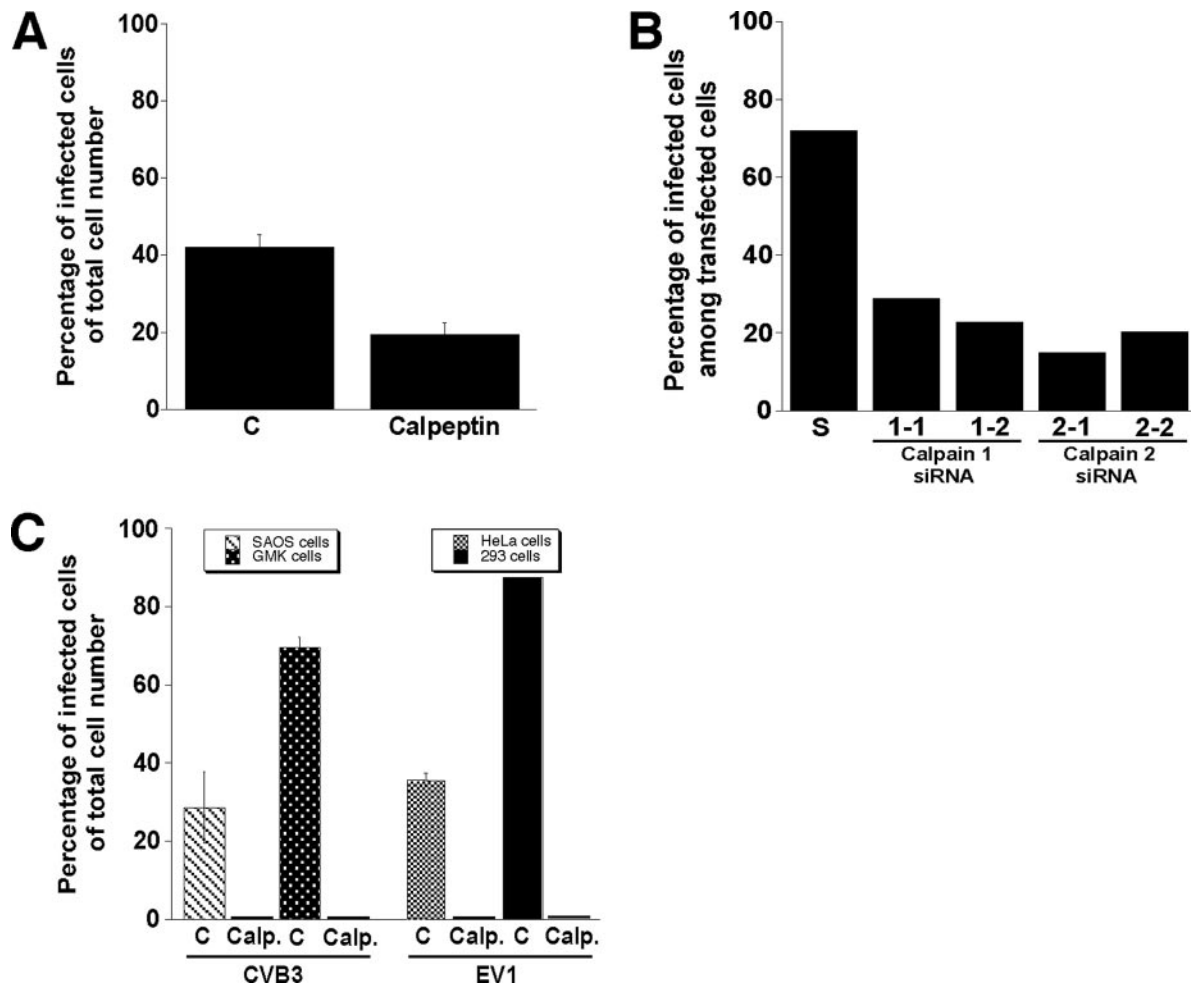
FIG. 2. Effect of calpain activity on HPEV1 and CVB3 infections. (A) The proportion of HPEV1-infected A549 cells in the absence or presence of calpeptin (140 μM), determined 6 h p.i. Error bars show the standard errors. C, untreated control. (B) The number of HPEV1-infected A549 cells 6 h p.i. among siRNA-positive cells was determined after transfection of calpain 1 (1-1 and 1-2) and 2 (2-1 and 2-2) siRNAs for 72 h prior to infection. A scrambled (S) siRNA was used as a control. (C) The proportion of CVB3-infected SAOS-α2β1 and GMK cells as well as EV1-infected HeLa MZ and 293 cells in the presence or absence of 140 μM calpeptin (Calp.). Error bars indicate the standard errors.

placed on ice for 5 min, diluted in Laemmli sample buffer, subjected to 10% PAGE, and analyzed by autoradiography.

siRNA-mediated protein depletion. Short interfering RNA (siRNA) duplexes were synthesized by Qiagen. The target sequences for human calpain 1 (GenBank accession number NM_005186) siRNA were CCG GAC CAT CCG CAA ATG GAA (calpain 1-1) and TAG GAT CAT CAG CAA ACA CAA (calpain 1-2). The target sequences for human calpain 2 (GenBank accession number NM_001748) siRNA were CCC GAG AAT ACT GGA ACA ATA (calpain 2-1) and TCG GCT GGA AAC GCT ATT CAA (calpain 2-2). A nontargeting scramble siRNA (Eurogentec) was used as a control. siRNAs were cotransfected into cells with a siGLO transfection indicator (Dharmacon) using Oligofectamine (Invitrogen) based on the manufacturer's instructions, with modifications. Briefly, 4 μl of Oligofectamine was added to 15 μl of serum-free DMEM (Gibco) and incubated for 10 min at room temperature. This mixture was combined with a second mixture containing a total of 20 μl of siRNA (20 μM) and 175 μl of serum-free DMEM and was incubated for an additional 20 min at room temperature before being added to cells in 30-mm dishes with glass coverslips. The cells were washed once and incubated with 0.8 ml DMEM, and the combined transfection mixture was added to cells, which then were incubated at 37°C for 4 h. After that, the cells were supplemented with a further 0.5 ml of DMEM containing 30% FCS. Transfected cells were incubated for 72 h before use in infections. The amount of infected cells among transfected cells was calculated based on the siGLO staining in the nucleus. Additionally, the RNA content was

assessed by TaqMan reverse transcription-PCR (RT-PCR) and was related to the amount of RNA produced by β-actin.

Quantitative RT-PCR. RNA was extracted from an SAOS-α2β1 cell pellet suspended in PBS using an automated nucleic acid isolation system (Nuclisens EasyMag; BioMerieux, Boxtel, The Netherlands). Positive- or negative-strand viral RNA was reverse transcribed in a reaction containing either the antisense (4−) or the sense (3+) primer, as described earlier (30). EV1 RNA from purified virions and the spectrophotometrically determined copy number were used as the quantitative standards. PCR was performed with a RotorGene 3000 instrument (Corbett Life Sciences, Sydney, Australia) using a reaction mixture containing QuantiTect SYBR green PCR mix (Qiagen), 600 nM of each of the primers, and the cDNA reaction product. Amplification steps were the following: 95°C for 15 min, 45 cycles of 95°C for 15 s, 65 to 55°C for 30 s (with a touch-down of 1°C/cycle for the first 10 cycles), and 72°C for 40 s. The specificity of the product was confirmed by melting curve analysis. The copy number of virus-specific RNA in the sample was determined from a plot of threshold cycles and copy numbers in standard dilutions.

RESULTS

Calpain inhibitors block EV1 infection in host cells. To test the hypothesis that host cell proteases are needed in the EV1

life cycle, we analyzed the role of calpains in the process. Calpains are proteases that can degrade cytoskeletal components and signaling proteins. Despite the facts that calpains are found in all human cells and that they seem to be essential for mouse development, their exact cellular functions are still under discussion. Here, we used an inhibitor for calpain 1 and 2, called calpeptin, and showed that it caused significant blocking of EV1 infection in cells (Fig. 1A). In confocal microscopy of both calpeptin-treated and control cells, EV1 capsid proteins could be found inside the cell in perinuclearly accumulated vesicles 2 h p.i. However, in calpeptin-treated cells EV1 remained mainly in these perinuclear vesicles up to 8 h p.i., while in nontreated cells the cytoplasm was full of newly synthesized viral capsid proteins (Fig. 1A). We confirmed the starting point of EV1 protein synthesis by using Western blotting with an antibody recognizing the viral RNA polymerase 3D (Fig. 1B). This EV1 protein was seen 4 h p.i. but not in samples taken 30 min earlier. No synthesis of the 3D protein was observed in cells treated with calpeptin (Fig. 1C). In order to measure the effect of calpain inhibition on the infectivity of EV1, a plaque titration also was performed. The sample treated with calpeptin produced no plaques, while the control sample produced 69 plaques (10^{-5} dilution) (Fig. 1D). The participation of calpain 1 and 2 in the replication cycle of EV1 was confirmed in the experiments, indicating that specific siRNAs (Fig. 1E) and chemical inhibitors for calpain 1 (*N*-acetyl-Leu-Leu-norleucinal) and calpain 2 (*N*-acetyl-Leu-Leu-methioninal) subtypes (Fig. 1F) also blocked the EV1 infection. The functionality of calpain siRNAs was tested. They downregulated calpain 1 and 2 expression at the mRNA level maximally by 85% (not shown). Downregulation of calpain 1 protein also was confirmed by Western blotting (not shown). An earlier study had indicated that several protease inhibitors may inhibit the proteolytic activity of poliovirus 2A^{pro} (24). However, here the selected protease inhibitors, namely, antipain, aprotinin, elastatinal, leupeptin, and trypsin inhibitor, had no significant effects on the EV1 life cycle (Fig. 1G). We also used metabolic labeling with [^{35}S]methionine to monitor the accumulation of viral proteins in the host cells. We did not detect the accumulation of any EV1-related protein with an unusual size that would have indicated that processing of EV1 proteins was affected (not shown).

Calpains also are required in HPEV1 and CVB3 infection. We also tested the effect of calpeptin on infection by two other picornaviruses, HPEV1 and CVB3. EV1 and CVB3 are closely related viruses representing the genus *Enterovirus*, while HPEV1 belongs to the genus *Parechovirus*. HPEV1 exhibits molecular properties distinct from those of other picornaviruses and exhibits unique features associated with the formation of the replication complex (20, 32). Unlike EV1, HPEV1 and CVB3 both are internalized by clathrin-dependent endocytosis (7, 17). Calpeptin could partially (54%) inhibit HPEV1 infection in A549 cells (Fig. 2A). The results were confirmed by using specific siRNAs for calpain 1 and 2 (Fig. 2B). The total inhibition of CVB3 infection by calpeptin was seen for SAOS-α2β1 and GMK cells (Fig. 2C). The effect of calpeptin on EV1 infection was confirmed in experiments with two other cell types, HeLa MZ and 293 cells (Fig. 2C). Thus, calpain inhibition disturbs the replication of at least two groups of picornaviruses regardless of the host cell line.
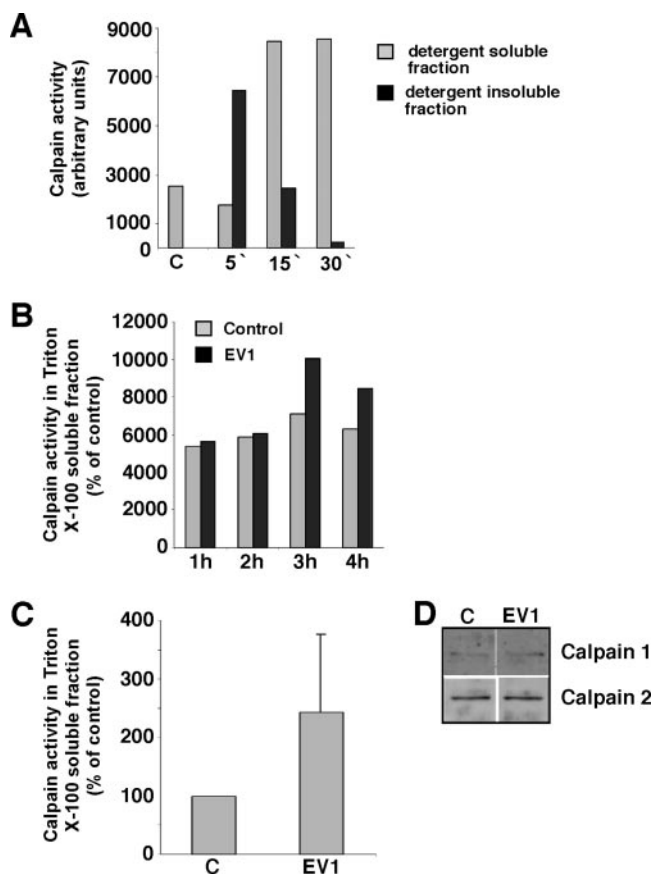

FIG. 3. Calpain activity assay. (A) Calpain activity was measured from detergent-soluble and -insoluble fractions of serum-starved SAOS-α2β1 cells after different periods of TPA (100 ng/ml) treatment. C, untreated control. (B) Calpain activity in the detergent-soluble fraction of uninfected and EV1-infected SAOS-α2β1 cells at the indicated time points p.i. (C) Calpain activity measured from EV1-infected SAOS-α2β1 cells 3 h p.i. The values are averages from four identical and separately performed experiments with detergent-soluble fractions. The error bar shows the standard error. (D) Protein levels of calpain 1 and calpain 2, detected by Western blot analysis 3 h p.i. using specific antibodies.

EV1 infection increases calpain activity. The ability of the EV1 replication cycle to control calpain activity was studied with activity assays (Fig. 3). A well-known activator of calpain activity, TPA, was used to test the assay system. TPA had no effect on the Triton X-100 solubility of the calpains (not shown), but it caused a remarkable increase in calpain activity, which was seen after 5 min in detergent-insoluble fractions and after 15 min in detergent-soluble fractions (Fig. 3A). EV1 infection could increase calpain activity 1.4-fold in detergent-soluble fractions 3 h p.i. (Fig. 3B, C), whereas no increase was seen in the expression level of calpain 1 or 2 (Fig. 3D). No activation of calpains was seen in detergent-insoluble fractions (not shown).

Calpains are essential at late stages of EV1 infection. The role of calpains was further tested at different stages of the EV1 life cycle. Calpeptin had no effect on the number of EV1 particles or α2β1 integrin clusters internalized (Fig. 4A). In a separate experiment, calpeptin was added at different time points after EV1 infection (Fig. 4B). Calpeptin could cause a
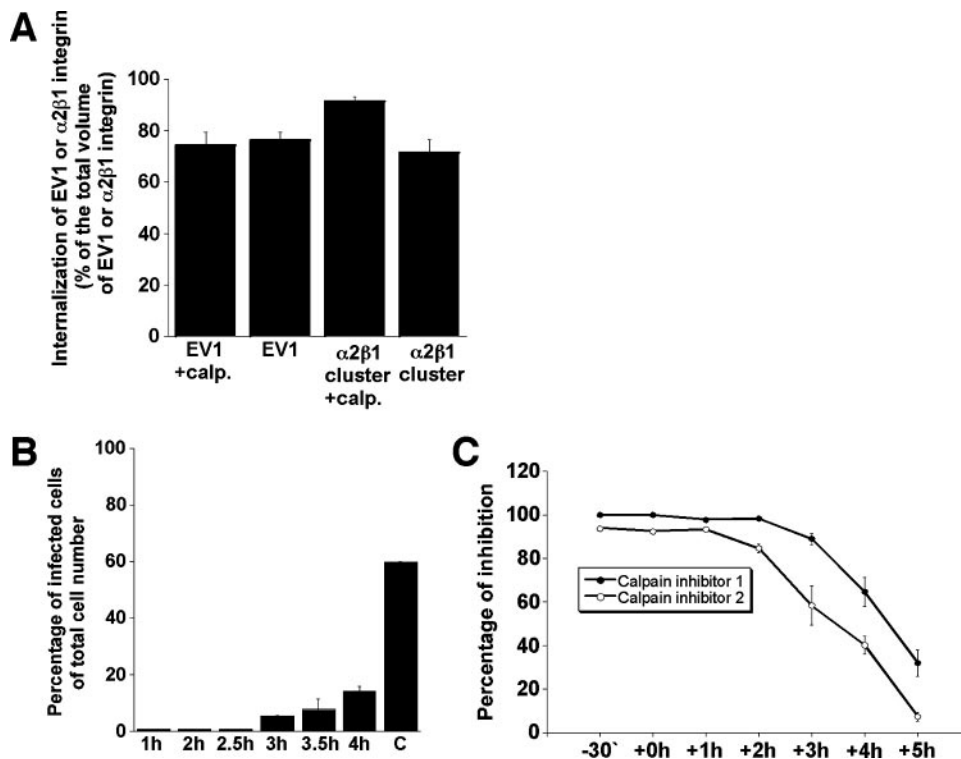
FIG. 4. Importance of calpains at late stages of EV1 infection. (A) The effect of calpeptin (calp.) on the internalization of EV1 or antibody-clustered α2β1 integrin in SAOS-α2β1 cells. (B) The blocking effect of calpeptin, added at the indicated time points p.i., on EV1 infection in SAOS-α2β1 cells. C, untreated control. (C) The inhibitory effects of calpain inhibitor 1 and calpain inhibitor 2 on EV1 infection in SAOS-α2β1 cells 6 h p.i. The inhibitors were added at the indicated time points p.i. Error bars show the standard errors.

total inhibition even when added at 2.5 h p.i. (Fig. 4B), confirming that it acts at late stages of the EV1 replication cycle. In further experiments, we also used selective synthetic inhibitors for calpain 1 and calpain 2, with similar results (Fig. 4C).

In confocal microscopy images, both calpain 1 and calpain 2 colocalized partially with GPI-AP-positive membrane domains (Fig. 5A) of SAOS-α2β1 cells, whereas no colocalization with caveolin-1 was seen (not shown). When the cells were extracted with detergent, calpain 1 was found mostly in Triton X-100-soluble fractions, whereas calpain 2 also was present in Triton X-100-insoluble fractions (Fig. 5B), as has been described previously (14, 19, 25). The intracellular localization of calpain 1 also was studied by flotation gradient centrifugation, and it was not found in detergent-resistant membrane fractions, in contrast to the GPI-APs or caveolin-1 (not shown). Thus, calpain 2 seems to be associated with detergent-insoluble membrane domains, whereas calpain 1 may be mainly cytosolic. EV1 internalization caused drastic relocalization of calpains. Both calpain 1 and calpain 2 became translocated into the intracellular vesicles containing the virus (Fig. 5C). The vesicles also seem to contain calpastatin, a cellular inhibitor of calpains (not shown). Calpeptin did not change the staining pattern of any of the proteins (not shown). The presence of calpain 1 and calpain 2 in EV1-containing vesicles also was confirmed by immunoelectron microscopy (Fig. 5D). EV1/α2β1-integrin-positive vesicles were visualized by allowing cells to internalize 10-nm protein A-gold particles linked with antibodies to α2β1 integrin that was clustered (35) simultaneously

with EV1 binding. The cells were treated with EV1 and antibodies in the same experiment to exclude the possibility that the virus might initiate a response differing from that of integrin signaling. Cell lysates were stained with antibodies specific to calpains and secondary antibodies carrying 5-nm protein A-gold particles. Calpains were seen on outer surfaces of membranes surrounding the internalized α2β1 clusters and intraluminal tubules (Fig. 5D). Our results indicate that both calpain 1 and calpain 2 already are associated with the EV1-containing vesicles during the early phases of entry.

Calpains are required in the replication of the EV1 RNA genome. Calpeptin also could prevent infection after microinjection of EV1 genomic RNA into the host cells (Fig. 6A). This confirms the idea that calpains are needed after the release of the EV1 genome into the cytoplasm. By using quantitative RT-PCR, we monitored the synthesis of negative and positive strands of EV1 RNA in the host cells. The copy numbers of both viral RNA strands started to increase between 3 and 4 h p.i., and after 4 h p.i. the increase was very fast (Fig. 6B to E). Calpeptin (Fig. 6B, C) and calpain inhibitors 1 and 2 (Fig. 6D and E) could prevent the replication of EV1 RNA. Finally, the effect of selected protease inhibitors on EV1 replication was quantified by RT-PCR. In contrast to calpeptin, protease inhibitors did not prevent the synthesis of RNA strands (Fig. 6F), confirming the specific role of calpains in the EV1 life cycle. We also tested the effect of calpeptin on the in vitro translation of EV1 RNA using a rabbit reticulocyte system. In the exper-
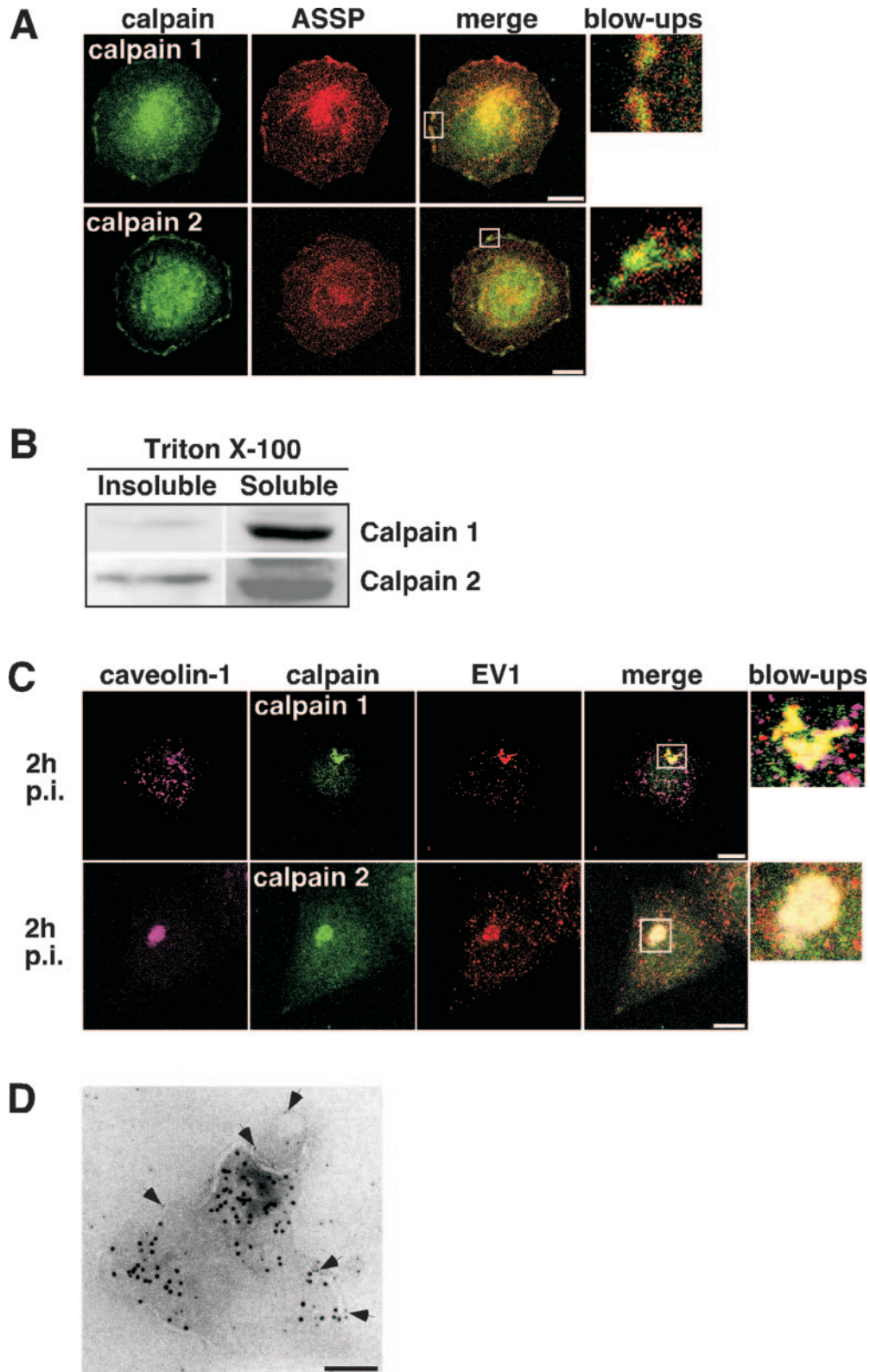
FIG. 5. Localization of calpain 1 and calpain 2 in intracellular EV1-containing vesicles. (A) Immunofluorescent labeling of calpain 1 and 2 (green) together with GPI-APs (aerolysin [ASSP]; red) in uninfected SAOS-α2β1 cells. White rectangles indicate the magnified portions (blow-ups). Bars, 10 μm. (B) Calpain 1 and 2 expression levels detected by Western blot analysis from detergent-soluble and -insoluble fractions of uninfected SAOS-α2β1 cells. (C) Immunofluorescent labeling of infected SAOS-α2β1 cells with EV1 antiserum together with antibodies against calpain 1 and 2 and caveolin-1. Confocal images are three-dimensional projections of scanned cells. White rectangles indicate the locations of the magnified portions. Bars, 10 μm. (D) An immunoelectron microscopy micrograph visualizing an intracellular vesicle containing protein A-gold-labeled (10 nm) antibody-induced α2β1 integrin clusters from SAOS-α2β1 cell lysates. The integrin clustering was done simultaneously with EV1 attaching to the cells, followed by incubation at 37°C for 30 min. The membranous location of calpain 2 (arrows) is indicated by immunostaining the cell lysates without permeabilization with anti-calpain 2 antibody linked to protein A-gold (5 nm). Bar, 100 nm.
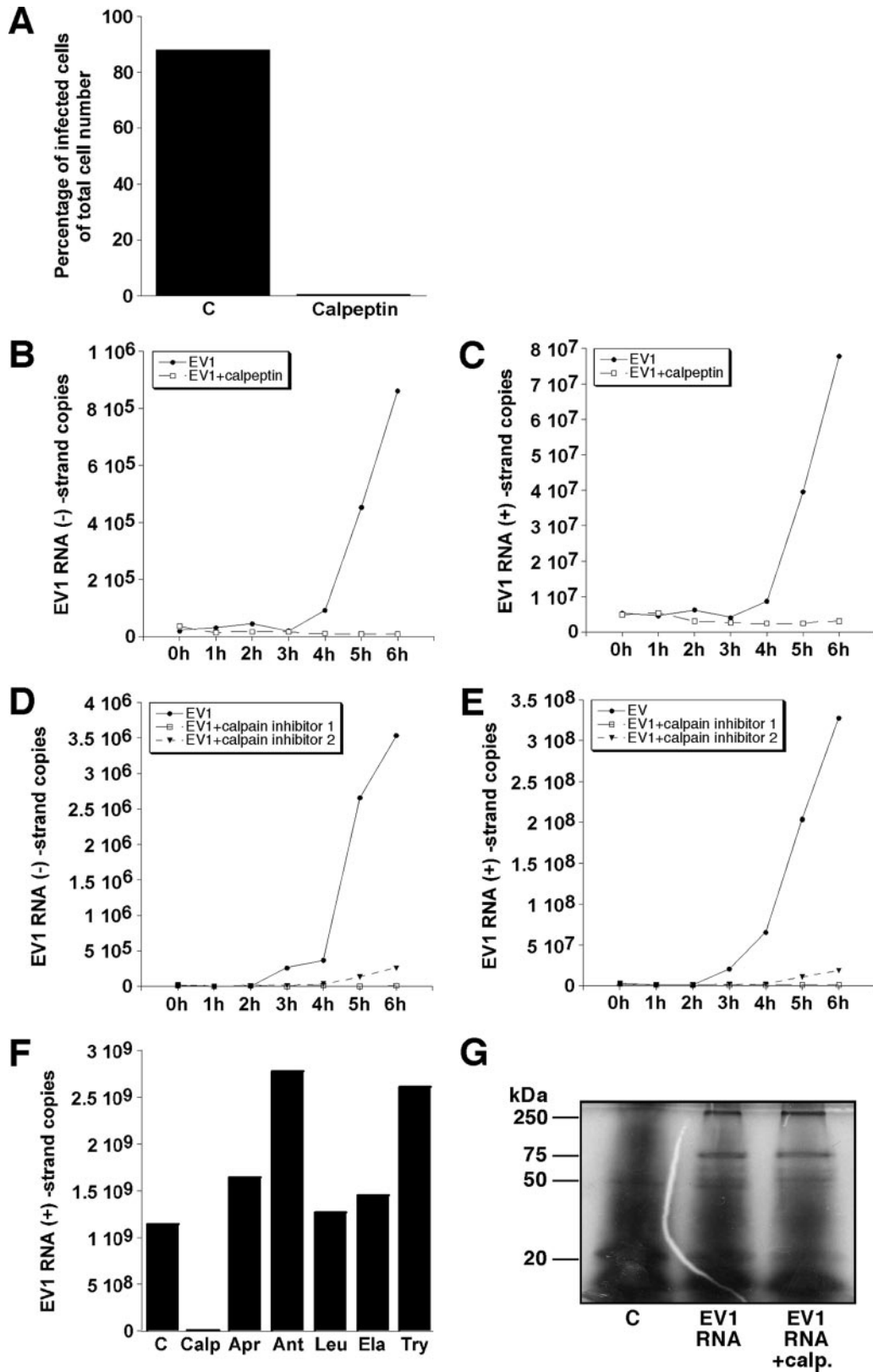
FIG. 6. Effect of calpain inhibition on EV1 RNA replication. (A) The proportion of infected cells, following EV1 RNA microinjection, in the presence or absence of calpeptin (140 μM) in SAOS-α2β1 cells 5 h p.i. The numbers of negative-strand (B) and genomic-strand (C) EV1 RNA copies analyzed by quantitative RT-PCR in the presence or absence of calpeptin (140 μM) at the indicated time points p.i. are shown. Negative-strand (D) and positive-strand (E) EV1 RNA copies in the presence or absence of calpain inhibitors 1 and 2 (130 μM) at the indicated time points p.i. also are shown. (F) The number of genomic-strand (positive) EV1 RNA copies analyzed by quantitative RT-PCR in the presence or absence of calpeptin (Calp; 140 μM) and protease inhibitors antipain (Ant; 500 μM), leupeptin (Leu; 500 μM), aprotinin (Apr; 5 U/ml), trypsin inhibitor (Try; 2 mM), and elastatinal (Ela; 250 μM) 6 h p.i. (G) The effect of calpeptin on in vitro cell-free translation of EV1 RNA in the rabbit reticulocyte system. The control (C) sample does not contain EV1 RNA.

iments, calpeptin could not inhibit the translation of viral proteins (Fig. 6G).

DISCUSSION

The mechanism of EV1 entry has many unique features not found in other viruses. The life cycle of EV1 is ruled by the biology of its cellular receptor, $\alpha2\beta1$ integrin. Natural ligands of $\alpha2\beta1$ integrin include various collagen subtypes. We have proposed that one EV1 pentamer can bind to up to five receptor molecules and cause receptor clustering (38). Integrin $\alpha2\beta1$ clustering alone is sufficient to induce lateral movement of the receptors on the cell surface, followed by rapid internalization into caveosomes (35). Calpains are abundant intracellular proteases regulating, e.g., cytoskeleton-membrane interactions and the activity of specific signaling proteins, such as focal adhesion kinase and small GTPases (13). Thus, calpains can participate in the regulation of integrin function and cellular trafficking. However, when we used a selective inhibitor for calpains, we could not see any effect on the internalization of EV1, suggesting that calpain-mediated reorganization of the cytoskeleton or degradation of actin-associated proteins (8, 9, 11) is not needed during the entry of EV1.

During the next 2 h after internalization, we saw the accumulation of both clustered $\alpha2\beta1$ integrin and EV1 into caveolin-1-positive vesicles that have a typical caveosome morphology in electron microscopy analysis (23). Here, we have shown that the structures are positive for calpain 2, and some calpain 1 also was detected using both confocal microscopy and immunoelectron microscopy. Furthermore, the vesicles seemed to be positive for a cellular inhibitor of calpains, namely, calpastatin. The accumulation of EV1 or calpains into these vesicles was not affected by calpeptin. Previous studies have shown that calpain 2, unlike calpain 1, accumulates into detergent-insoluble membranes or lipid rafts (14, 19, 25). We could see both calpains in caveosome-like vesicles, but our results were in agreement with the idea that calpain 2 predominates there, whereas calpain 1 is more import in the cytoplasm. We do not know whether the EV1-containing, caveosome-like vesicles contain natural targets of calpain-mediated proteolysis. We could not find any degradation of caveolin-1 after incubation with purified calpain 1 or 2, and the capsid proteins in the virus particles were not sensitive to calpains (P. Upla, unpublished data), but interestingly, calpains could degrade $\alpha2\beta1$ integrin in vitro (L. Nissinen, unpublished data). Previous studies have indicated that calpains can degrade cytoskeletal proteins, which may make the cellular membranes unstable and leaky (6, 8, 21, 27). Our studies do not exclude the possibility that similar events take place in caveosomes, but the calpains seem to play a more critical role at a later stage of the EV1 life cycle, and they may modify cellular membranes in a manner that disturbs the formation of functional replication complexes.

The EV1 genome is released into the cytoplasm, where the replication of viral RNA is initiated. Our results suggest that cytoplasmic calpain activity is essential for the EV1 life cycle after this stage. An earlier study indicated that several protease inhibitors, including calpain inhibitor 1, may inhibit the proteolytic activity of poliovirus 2A^{pro} (24). In our studies here, the other protease inhibitors had no effect on EV1 infections, and importantly, the results with calpain 1 and 2 siRNAs con-

firmed that the described effect was not due to the unspecific inhibition of viral proteases. In metabolic labeling experiments, we did not detect any unusual EV1-related proteins that could have indicated that processing was affected.

EV1 also increased calpain activity in the cytoplasm. We have tested the hypothesis that the intracellular Ca^{2+} concentration is involved in the regulation of calpain activity during EV1 infection and have shown that a cytosolic Ca^{2+} concentration is increased by 1 h p.i., and the increase can be detected for approximately 4 h (M. Karjalainen, unpublished data). Furthermore, inhibitors of Ca^{2+} relocation, such as Bapta AM, thapsigarcin, and nifedipin, inhibited EV1 infection (M. Karjalainen, unpublished). Thus, EV1 may increase the Ca^{2+} concentration in the cytosol and contribute to the general increase in calpain activity in the cytoplasm.

Calpeptin also could inhibit the infection by two other picornaviruses, HPEV1 and CVB3, that both utilize a clathrin-dependent endocytosis route (7, 17). In the case of HPEV1 infection, the inhibitory effect of calpeptin was only partial, whereas CVB3 infection was completely prevented. The mechanisms used for the replication may be more similar between the closely related CVB3 and EV1, explaining the analogous effects of calpain inhibition. Importantly, our results indicate that calpeptin also inhibits the replication of other single-stranded RNA viruses. Furthermore, EV1 RNA microinjected into cytoplasm could not cause infection in the presence of calpeptin. We suggest that the formation of the replication complex or its function is dependent on calpain activity. This also was evident in the experiments measuring the accumulation of positive- and negative-strand EV1 RNA synthesis in the host cells. We also have tested the effect of calpeptin on the in vitro translation of EV1 RNA. In the experiments, calpeptin could not inhibit the translation of viral proteins.

To conclude, calpains are very abundant cellular proteases, but their physiological role had remained enigmatic until it was recently proposed that they might regulate important cellular functions, such as cytoskeletal connections to membranes, cell signaling, and apoptosis (13). Our results show that calpain activity is critical for the life cycle of EV1 and important in the multiplication of the viral RNA genome.

REFERENCES

1. **Arthur, J. S., and C. Crawford.** 1996. Investigation of the interaction of m-calpain with phospholipids: calpain-phospholipid interactions. Biochim. Biophys. Acta **1293:**201–206.
2. **Arthur, J. S., J. S. Elce, C. Hegadorn, K. Williams, and P. A. Greer.** 2000. Disruption of the murine calpain small subunit gene, Capn4: calpain is essential for embryonic development but not for cell growth and division. Mol. Cell. Biol. **20:**4474–4481.
3. **Auvinen, P., M. J. Mäkelä, M. Roivainen, M. Kallajoki, R. Vainionpää, and T. Hyypiä.** 1993. Mapping of antigenic sites of coxsackievirus B3 by synthetic peptides. APMIS **101:**517–528.
4. **Azam, M., S. S. Andrabi, K. E. Sahr, L. Kamath, A. Kuliopulos, and A. H. Chishti.** 2001. Disruption of the mouse μ-calpain gene reveals an essential role in platelet function. Mol. Cell. Biol. **21:**2213–2220.

5. **Bergelson, J. M., M. P. Shepley, B. M. Chan, M. E. Hemler, and R. W. Finberg.** 1992. Identification of the integrin VLA-2 as a receptor for echovirus 1. Science **255:**1718–1720.

6. **Bialkowska, K., S. Kulkarni, X. Du, D. E. Goll, T. C. Saido, and J. E. Fox.** 2000. Evidence that β3 integrin-induced Rac activation involves the calpain-dependent formation of integrin clusters that are distinct from the focal complexes and focal adhesions that form as Rac and RhoA become active. J. Cell Biol. **151:**685–696.

7. **Chung, S. K., J. Y. Kim, I. B. Kim, S. I. Park, K. H. Paek, and J. H. Nam.** 2005. Internalization and trafficking mechanisms of coxsackievirus B3 in HeLa cells. Virology **333:**31–40.

8. **Cooray, P., Y. Yuan, S. M. Schoenwaelder, C. A. Mitchell, H. H. Salem, and S. P. Jackson.** 1996. Focal adhesion kinase (pp125FAK) cleavage and regulation by calpain. Biochem. J. **318:**41–47.

9. **Cuevas, B. D., A. N. Abell, J. A. Witowsky, T. Yujiri, N. L. Johnson, K. Kesavan, M. Ware, P. L. Jones, S. A. Weed, R. L. DeBiasi, Y. Oka, K. L. Tyler, and G. L. Johnson.** 2003. MEKK1 regulates calpain-dependent proteolysis of focal adhesion proteins for rear-end detachment of migrating fibroblasts. EMBO J. **22:**3346–3355.

10. **Debiasi, R. L., M. K. Squier, B. Pike, M. Wynes, T. S. Dermody, J. J. Cohen, and K. L. Tyler.** 1999. Reovirus-induced apoptosis is preceded by increased cellular calpain activity and is blocked by calpain inhibitors. J. Virol. **73:**695–701.

11. **Dedieu, S., S. Poussard, G. Mazeres, F. Grise, E. Dargelos, P. Cottin, and J. J. Brustis.** 2004. Myoblast migration is regulated by calpain through its involvement in cell attachment and cytoskeletal organization. Exp. Cell Res. **292:**187–200.

12. **Fivaz, M., F. Vilbois, S. Thurnheer, C. Pasquali, L. Abrami, P. E. Bickel, R. G. Parton, and F. G. van der Goot.** 2002. Differential sorting and fate of endocytosed GPI-anchored proteins. EMBO J. **21:**3989–4000.

13. **Goll, D. E., V. F. Thompson, H. Li, W. Wei, and J. Cong.** 2003. The calpain system. Physiol. Rev. **83:**731–801.

14. **Hood, J. L., B. B. Logan, A. P. Sinai, W. H. Brooks, and T. L. Roszman.** 2003. Association of the calpain/calpastatin network with subcellular organelles. Biochem. Biophys. Res. Commun. **310:**1200–1212.

15. **Hyypiä, T., C. Horsnell, M. Maaronen, M. Khan, N. Kalkkinen, P. Auvinen, L. Kinnunen, and G. Stanway.** 1992. A distinct picornavirus group identified by sequence analysis. Proc. Natl. Acad. Sci. USA **89:**8847–8851.

16. **Ivaska, J., H. Reunanen, J. Westermarck, L. Koivisto, V. M. Kähäri, and J. Heino.** 1999. Integrin α2β1 mediates isoform-specific activation of p38 and upregulation of collagen gene transcription by a mechanism involving the α2 cytoplasmic tail. J. Cell Biol. **147:**401–416.

17. **Joki-Korpela, P., V. Marjomäki, C. Krogerus, J. Heino, and T. Hyypiä.** 2001. Entry of human parechovirus 1. J. Virol. **75:**1958–1967.

18. **Kalamvoki, M., and P. Mavromara.** 2004. Calcium-dependent calpain proteases are implicated in processing of the hepatitis C virus NS5A protein. J. Virol. **78:**11865–11878.

19. **Kifor, O., I. Kifor, F. D. Moore, Jr., R. R. Butters, Jr., and E. M. Brown.** 2003. m-calpain colocalizes with the calcium-sensing receptor (CaR) in caveolae in parathyroid cells and participates in degradation of the CaR. J. Biol. Chem. **278:**31167–31176.

20. **Krogerus, C., O. Samuilova, T. Pöyry, E. Jokitalo, and T. Hyypiä.** 2007. Intracellular localization and effects of individually expressed human parechovirus 1 non-structural proteins. J. Gen. Virol. **88:**831–841.

21. **Kulkarni, S., D. E. Goll, and J. E. Fox.** 2002. Calpain cleaves RhoA generating a dominant-negative form that inhibits integrin-induced actin filament assembly and cell spreading. J. Biol. Chem. **277:**24435–24441.

22. **Leverrier, S., A. Vallentin, and D. Joubert.** 2002. Positive feedback of protein kinase C proteolytic activation during apoptosis. Biochem. J. **368:**905–913.

23. **Marjomäki, V., V. Pietiäinen, H. Matilainen, P. Upla, J. Ivaska, L. Nissinen, H. Reunanen, P. Huttunen, T. Hyypiä, and J. Heino.** 2002. Internalization of echovirus 1 in caveolae. J. Virol. **76:**1856–1865.

24. **Molla, A., C. U. Hellen, and E. Wimmer.** 1993. Inhibition of proteolytic activity of poliovirus and rhinovirus 2A proteinases by elastase-specific inhibitors. J. Virol. **67:**4688–4695.

25. **Morford, L. A., K. Forrest, B. Logan, L. K. Overstreet, J. Goebel, W. H. Brooks, and T. L. Roszman.** 2002. Calpain II colocalizes with detergent-insoluble rafts on human and Jurkat T-cells. Biochem. Biophys. Res. Commun. **295:**540–546.

26. **Papp, B., and R. A. Byrn.** 1995. Stimulation of HIV expression by intracellular calcium pump inhibition. J. Biol. Chem. **270:**10278–10283.

27. **Pfaff, M., X. Du, and M. H. Ginsberg.** 1999. Calpain cleavage of integrin beta cytoplasmic domains. FEBS Lett. **460:**17–22.

28. **Saido, T. C., M. Shibata, T. Takenawa, H. Murofushi, and K. Suzuki.** 1992. Positive regulation of μ-calpain action by polyphosphoinositides. J. Biol. Chem. **267:**24585–24590.

29. **Salonen, A., T. Ahola, and L. Kääriäinen.** 2005. Viral RNA replication in association with cellular membranes. Curr. Top. Microbiol. Immunol. **285:**139–173.

30. **Säntti, J., T. Hyypiä, and P. Halonen.** 1997. Comparison of PCR primer pairs in the detection of human rhinoviruses in nasopharyngeal aspirates. J. Virol. Methods **66:**139–147.

31. **Sato, K., and S. Kawashima.** 2001. Calpain function in the modulation of signal transduction molecules. Biol. Chem. **382:**743–751.

32. **Stanway, G., and T. Hyypiä.** 1999. Parechoviruses. J. Virol. **73:**5249–5254.

33. **Suzuki, K., S. Hata, Y. Kawabata, and H. Sorimachi.** 2004. Structure, activation, and biology of calpain. Diabetes **53**(Suppl. 1)**:**S12–S18.

34. **Teranishi, F., Z. Q. Liu, M. Kunimatsu, K. Imai, H. Takeyama, T. Manabe, M. Sasaki, and T. Okamoto.** 2003. Calpain is involved in the HIV replication from the latently infected OM10.1 cells. Biochem. Biophys. Res. Commun. **303:**940–946.

35. **Upla, P., V. Marjomäki, P. Kankaanpää, J. Ivaska, T. Hyypiä, F. G. Van Der Goot, and J. Heino.** 2004. Clustering induces a lateral redistribution of α2β1 integrin from membrane rafts to caveolae and subsequent protein kinase C-dependent internalization. Mol. Biol. Cell **15:**625–636.

36. **van Kuppeveld, F. J., J. G. Hoenderop, R. L. Smeets, P. H. Willems, H. B. Dijkman, J. M. Galama, and W. J. Melchers.** 1997. Coxsackievirus protein 2B modifies endoplasmic reticulum membrane and plasma membrane permeability and facilitates virus release. EMBO J. **16:**3519–3532.

37. **Vuorinen, T., R. Vainionpää, H. Kettinen, and T. Hyypiä.** 1994. Coxsackievirus B3 infection in human leukocytes and lymphoid cell lines. Blood **84:**823–829.

38. **Xing, L., M. Huhtala, V. Pietiäinen, J. Käpylä, K. Vuorinen, V. Marjomäki, J. Heino, M. S. Johnson, T. Hyypiä, and R. H. Cheng.** 2004. Structural and functional analysis of integrin α2I domain interaction with echovirus 1. J. Biol. Chem. **279:**11632–11638.

39. **Zatz, M., and A. Starling.** 2005. Calpains and disease. N. Engl. J. Med. **352:**2413–2423.